Tire models used in accident reconstruction vehicle motion simulation

Raymond M. Brach, University of Notre Dame, Brach Engineering,
R. Matthew Brach, Brach Engineering

Abstract

Various vehicle dynamic simulation software programs have been developed for use in reconstructing accidents. Typically these are used to analyze and reconstruct preimpact and postimpact vehicle motion. These simulation programs range from proprietary programs to commercially available packages. While the basic theory behind all simulations is Newton's laws of motion, some component modeling techniques differ from one program to another. This is particularly true of the modeling of tire force mechanics. Since tire forces control the vehicle motion predicted by a simulation, the tire mechanics model is a critical feature in simulation use, performance and accuracy. This is particularly true for accident reconstruction applications where vehicle motions can occur over wide ranging kinematic wheel conditions. Therefore a thorough understanding of the nature of tire forces is a necessary aspect of the proper formulation and use of a vehicle dynamics program.

This paper includes a discussion of tire force mechanics, definitions of terms, modeling of individual tire force components and tire forces for combined braking and steering currently used in simulation software for reconstruction of accidents. The paper discusses the difference between a tire force ellipse and the friction ellipse. Equations are presented for five tire force models from three different simulation programs. Each model uses a different method for computing tire force components and combined braking and steering. Some tire force models begin with a specified level of braking force and use the friction ellipse to determine the corresponding steering force; this produces a resultant tire force equal in magnitude to full skidding for combined steering and braking.

Three dimensional surface plots of the calculated forces are presented of all of the models. This allows for a visual comparison of the combined forces over a full range of the longitudinal and lateral tire slip variables.

Introduction

Tire Models: Beside helping to provide a smooth ride, the main function of an automotive pneumatic tire is to transmit forces with components, F_x, F_y, F_z, and moments, M_x, M_y, M_z, in three mutually perpendicular directions for vehicle directional control. This important role of tires has made tire behavior the subject of continuous study (and performance improvement) for nearly 80 years. Numerous tests have been conducted and mathematical models have been developed in an attempt to understand and predict these forces. Tire models have been divided into four different classifications [Pacejka]: 1) those that use a complex physical model, 2) those using a simple physical model, 3) models using similarity methods, and 4) models based solely on experimental data, so-called empirical models. Physical models are those intended to model tire performance (rather than vehicle performance). Physical models are concerned with such things as tire wear, temperature, traction, life, cost, etc. They have parameters such as construction, materials, loads, inflation pressure, geometry, tread design, speed, and so on. Complex physical models typically use finite element modeling techniques. Finite element models of tires are of particular use when considering the interaction between the tire and road irregularities and investigations into the friction between the road and the tire within the footprint of the tire [Tonuk and Unlusoy, Heschler, et al.]. Models based on similarity methods were useful early in the tire force model development process but have found less use recently as they have been superceded by the utility afforded by other models. Such methods are covered by Pacejka [Pacejka].

The two remaining model classifications, the simple physical model and the empirical models, are the two most prevalent used in the understanding and prediction of tire forces. They relate the physical and kinematical properties of tires to the development of tractive forces at the contact between the tire and the roadway surface. One of the most widely used simple physical model is the brush model. Brush models have been improved and developed over the recent years [Gäfvert & Svedenius] but have not yet found their way into dynamic simulation programs applied to accident reconstruction. A thorough coverage of the brush model is included in Pacejka [Pacejka].

The remaining tire model classification is the empirical tire model. Such models are also referred to as semi-empirical tire models in many references [Pacejka, Guo and Ren]. These models deal exclusively with the steady-state behavior of a tire. Treatment of the transient behavior of the tire, for example oscillatory response, response lag and wheel unbalance, is given elsewhere

[Pacejka, Allen, et al.]. Empirical models employ mathematical functions capable of emulating the highly nonlinear behavior of the forces generated by the tires that is observed in experiment force data. These mathematical functions can range from straight line segment approximations to nonlinear functions that contain numerous coefficients based on experimental data and determined by curve-fitting routines. The principal use of these models is in the prediction of tire forces for vehicle dynamics simulation software. Many of these empirical models exist [Pacejka, Guo, Gäfvert, Hirschberg, Brach & Brach (2000), Pottinger, et al.]. This is the type of model examined in this paper.

Tire forces can be separated into a longitudinal force component (braking and driving) and a lateral force component (steering/cornering). The longitudinal tire force typically is mathematically expressed (modeled) and measured as a function of a variable called wheel slip. In some cases the longitudinal force is modeled simply by a prescribed force level, sometimes expressed as a fraction of the normal force. The lateral tire force is mathematically expressed (modeled) and measured as a function of a variable called the sideslip angle, or simply slip angle. A third, distinct, feature of a tire force model is the method of properly combining these two force components for conditions of combined braking (wheel slip) and steering (sideslip). Other forces and moments exist at the tire-road interface that are important for vehicle handling and design but are not considered here. Effects such as self-aligning torque, camber steer, conicity steer, ply steer, etc. are usually neglected for accident reconstruction applications.

It must be pointed out that the tire models discussed here are referred to as steady-state models. Such models do not directly model transient behavior of the tires such as the effects of relaxation and hysteresis.

Vehicle Dynamic Simulation: The use of vehicle dynamics models in the field of accident reconstruction to simulate vehicle motion has evolved steadily over the last few decades. Initially, the options of the reconstructionist were limited to the vehicle dynamics capabilities of the variants with the US government-funded SMAC & HVOSM [McHenry, Segal] computer programs being the most readily available options. Even today, simulation software appears to be underutilized in the field as some reconstructionists continue to use simplified methods in attempts to address complex motion of a vehicle based on assumptions of constant deceleration [Fricke 1, Fricke 2, Orlowski, Daily, et al., Martinez] and even concepts such as “point mass rotational friction” [Keifer, et al. (2005) and Keifer, et al. (2007)]. Various simulation programs are available to the accident reconstructionist in the form of computer-based vehicle dynamics programs and are becoming an integral part of various accident reconstruction software [PC-Crash, HVE, VCRware]. These are vehicle dynamic programs developed from within the accident reconstruction community and are particularly suited to the needs of that field. Other, more complex vehicle dynamic software is also available [VDANL, Car-Sim, ADAMS]. While the latter software can be used in accident reconstruction work, their complexity is better suited for vehicle development applications.

The basic premise behind all of the variations of vehicle dynamics simulation programs is essentially the same: a user provides initial conditions (position, orientation, velocity) for the vehicle, the vehicle-specific geometry, the vehicle physical parameters (including tire parameters), and any time-dependent parameters (such as steering input, braking/acceleration, etc.). The program integrates the differential equations of motion of the vehicle (and semitrailer) to predict the motion as a function of time for the given input conditions. The needs that the accident reconstruction community has for a simulation program can differ from other users of vehicle dynamics programs. Such needs include the ability to capture the dynamics of the vehicle over a wide range of motion and vehicle conditions such as damaged or altered wheelbase and/or track width, one or more wheels that are fully or partially locked due to crash damage, large initial yaw rates following an impact, etc. In contrast, vehicle design and development work typically use vehicle dynamics to study the performance of a vehicle in its as-designed condition and operation.

Comparisons have been made [Han and Park] between EDVAP [HVE], PC-Crash (linear tire model) [PC-Crash] and a proprietary simulation program. These comparisons consisted of three categories of initial conditions that result in three different types of postimpact motion. Category 1 uses initial conditions with a relatively high yaw velocity. The resulting vehicle motion showed that the yaw velocity decreased to near zero and the vehicle continued with a translational motion (rollout). Category 2 uses initial conditions that resulted in a nonzero yaw velocity that was maintained until rest (spinout). Category 3 uses initial conditions that result in the vehicle experiencing a moderate yaw velocity and translation. The results showed that the largest differences between EDVAP and PC-Crash occurred for the initial conditions of Category 1. Only small differences were found for Categories 2 and 3. The following work focuses on differences between tire force models in the different simulation programs. All three models use the friction ellipse to compute combined tire forces.

In all cases, tire force accuracy is of considerable importance to the users of the simulation software. To a great extent, simulation accuracy depends on the ability of the tire model to predict accurately the forces generated by each of the vehicle’s tires acting in the plane of the roadway. Other than aerodynamic forces, it is the tire forces acting at the tire-road contact patches that produce the motion of the vehicle.

This paper focuses on the tire models used by three currently available simulation programs, PC-Crash, HVE and VCRware. These all have the capability to simulate motion in at least two dimensions and can use a rigid vehicle suspension system. Some have more general capabilities such as three dimensional motion but these features are not considered here. The tire models used by each of these software programs is described in detail. Tire moments are excluded here as they typically are not significant for purposes of accident reconstruction.

NOTATION, ACRONYMS AND DEFINITIONS

• **BNP**: Bakker-Nyborg-Pajecka equations (also known as the Magic Formula) [Pacejka]
• ***C_α***: lateral tire force coefficient (also cornering coefficient),
• **Cornering stiffness:** see C_α
• **Cornering compliance:** $1/C_\alpha$
• **EDSMAC4**: simulation software [HVE],
• **frictional drag coefficient**: average, constant value of the coefficient of friction of a fully sliding tire over a surface under given conditions (wet, dry, asphalt, concrete, gravel, ice, etc.) appropriate to an application,
• **friction circle**: the friction ellipse when $\mu_x = \mu_y$,
• **friction ellipse**: an idealized curve with coordinates consisting of the longitudinal and lateral tire force components that defines the transition of the resultant tire force from slip to the condition of full sliding,
• **$F_x(s)$**: an equation with a single independent variable, s, that models a longitudinal tire force *for no steering, $\alpha = 0$*,
• **$F_y(\alpha)$**: an equation with a single independent variable, α, that models a lateral force *for no braking, $s = 0$*,
• **$F_x(\alpha,s) = F_x[F_x(s),F_y(\alpha),\alpha,s]$**: an equation with two independent variables, (α,s), that models a longitudinal tire force component *for combined braking and steering*,
• **$F_y(\alpha,s) = F_y[F_x(s),F_y(\alpha),\alpha,s]$**: an equation of two independent variables, (α,s), that models a lateral tire force component *for combined braking and steering*,
• **F_z**: wheel normal force,
• **full sliding**: a condition when the combined slip variables (α,s) give a resultant tire force equal to μF_z, the same as *skidding*; see *sliding*,
• **HVOSM:** Highway Vehicle Object Simulation Model
• **lateral (side, cornering, steering)**: in the direction of the y axis of a tire's coordinate system,
• **longitudinal (forward, rearward, braking, accelerating, driving)**: in the direction of the x axis of a tire's coordinate system,• **F_b**: input value for the braking or acceleration force, PC-Crash, if $F_b > 0$, tire force is positive (acceleration), if $F_b < 0$, tire force is negative (braking),
• **m-smac**: simulation software [m-smac]
• **NCB**: Nicolas-Comstock-Brach equations [Brach & Brach 2000, 2005]
• **PC-Crash**: simulation software [PC-Crash],
• **rollout**: translational motion alone of a vehicle that continues following spinout,
• **sideslip:** see α,
• **SIMON**: **SI**mulation **MO**del **N**onlinear [HVE]
• **sliding**: the condition of a moving wheel and tire locked from rotating ($s = 1$), or moving sideways ($\alpha = \pi/2$),
• ***s***: longitudinal wheel slip,
• **slip velocity**: the velocity relative to the ground of the center of a tire at the contact patch,
• **slip angle**: see sideslip angle, α,
• **SMAC**: Simulation Model of Automobile Collisions [McHenry]
• **spinout**: motion of a vehicle that includes both translation and yaw rotation,
• ***T***: an input value for the braking or acceleration force, SMAC,
if $T > 0$, tire force is positive (acceleration), if $T < 0$, tire force is negative (braking),
• **VCRware**: simulation software [VCRware],
• **V_x, V_y**: components of the velocity of a wheel's hub expressed in the tire's coordinate system,
• **V_p**: slip velocity of a tire at point P of the tire patch.
• **wheel slip**: see s,
• ***x-y-z***: orthogonal tire coordinates where x is in the direction of the tire's heading and z is perpendicular to the tire's contact patch (see Fig 1),
• **yaw:** vehicle rotation about a vertical axis
• **α**: tire slip angle (also, tire sideslip angle and lateral sideslip angle),
• **β_p**: angle of a tire's slip velocity relative to the tire's x axis and angle of the resultant force parallel to the road plane (see Fig 2),
• **β**: angle relative to the x axis of the resultant tire force (see Fig 2),
• **$\bar{\beta}$** : nondimensional slip angle, Eq 45 & 50, SMAC,
• **μ_x**: tire-surface frictional drag coefficient measured for full sliding in the longitudinal direction, $s = 1$, $\alpha = 0$,
• **μ_y**: tire-surface frictional drag coefficient measured for full sliding in the lateral direction, $\alpha = \pi/2$.

TIRE KINEMATICS

Two kinematic variables typically are used with tire force models and with the measurement of tire forces. These are the sideslip angle, α, and the longitudinal wheel slip, s. Sideslip angle, or slip angle, defined at the wheel hub, is illustrated in Fig 1 and is defined as

$$\alpha = \tan^{-1}(V_y / V_x) \tag{1}$$

Wheel slip can have different definitions [Brach & Brach (2000), Pacejka]. The one used here is such that $0 \le s \le 1$, where

$$s = \frac{V_x - R\omega}{V_x} \tag{2}$$

Figures 1 and 2 show the tire slip velocity components $V_{Px} = V_x - R\omega$ and $V_{py} = V_y$. Note that the resultant vector velocity, V, at the wheel hub and resultant slip velocity, V_p, at the contact patch center differ both in magnitude and direction. The slip velocity, V_p, is the velocity of the point P relative to the road surface. Also, the direction of the resultant force, F, and the slip velocity, V_p, generally differ. For no steering, the longitudinal (braking, accelerating) tire force component, $F_x(s)$, typically is expressed mathematically as a function of the wheel slip alone. Similarly, for no braking, the lateral (cornering, steering) force component, $F_y(\alpha)$, typically is expressed mathematically as a function of the sideslip angle alone.

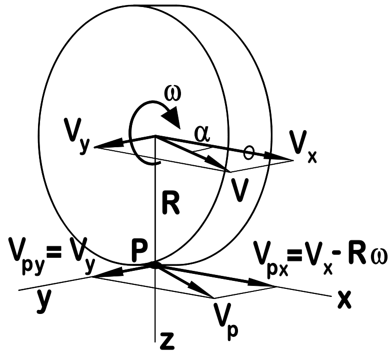

Figure 1. Wheel/tire velocities

FRICTION ELLIPSE, TIRE FORCE ELLIPSE

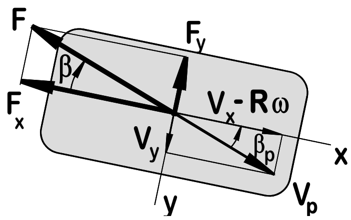

Figure 2. Tire patch velocity and force components.

The x-y tire coordinate system and velocities of a rotating wheel are illustrated in Fig 1. In an ideal sense a tire can be slipping at the tire-road interface and be providing controlled longitudinal and lateral tire force components. This condition occurs when the resultant tire force lies within the friction (limit) ellipse, Fig 3. However, when control is lost, a condition of skidding (full sliding) is reached where the tire force reaches its sliding value, μF_z, and the direction of the resultant force opposes the velocity, V_p. This is when the resultant tire force lies on the friction (limit) ellipse. Some, such as the Nicolas-Comstock model [Brach & Brach, 2000], define an operating tire force ellipse, Fig 3. The tire force components for combined braking and steering $F_x = F_x(\alpha,s)$, $F_y = F_y(\alpha,s)$ and resultant, $F = F(\alpha,s)$, are illustrated over a tire-road contact patch in Fig 2. Ideally the force components form a force ellipse where the abscissa is the longitudinal tire force component, $F_x(\alpha,s)$, and ordinate is the lateral tire force component, $F_y(\alpha,s)$. The equation of the tire force ellipse is given by Eq 3, or in a more concise form in Eq 4 [Brach and Brach, 2005]. The resultant force is $F(\alpha,s) = \sqrt{F_x^2(\alpha,s) + F_y^2(\alpha,s)}$. As shown in Fig 3, the $F_x(\alpha,s)$ axis (abscissa) represents braking alone (i.e., $\alpha = 0$). The $F_y(\alpha,s)$ axis (ordinate) represents steering alone (i.e., $s = 0$). Each point of the friction ellipse's interior is a point with slip values (α,s) for combined steering and braking that represents driver control, expressed mathematically by Eq 5. The point $F_x(s)|_{s=1} = \mu_x F_z$ on the abscissa represents locked wheel skidding for braking alone. The point, $F_y(\alpha)|_{\alpha=\pi/2} = \mu_y F_z$, on the ordinate represents a vehicle wheel sliding laterally. Note that this formulation allows for different frictional drag coefficients, μ_x and μ_y, in the x and y directions, respectively. Full sliding of the tire under any combination of α and s occurs if the resultant tire force reaches the friction ellipse, $F(\alpha,s) = \mu F_z$, where [Brach & Brach (2000)] the frictional drag coefficient, μ is given by Eq 6. For a given normal force, F_z, points outside the friction ellipse cannot be reached because the friction force is limited by μF_z. If $\mu_x = \mu_y$, then the tire force ellipse become a circle and the friction ellipse becomes a friction circle.

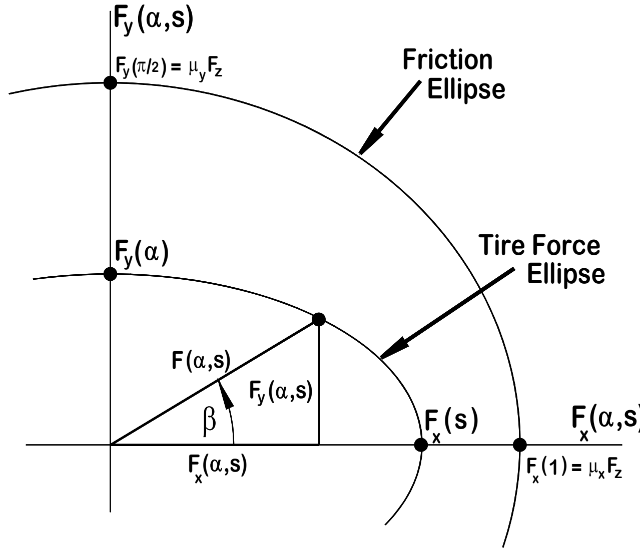

Figure 3. Friction (Limit) Ellipse and Tire Force Ellipse.

Model equations that determine the functions $F_x(\alpha,s)$ and $F_y(\alpha,s)$ for combined steering and braking (such as shown in Fig 3 as a tire force ellipse) must be found independently from the steering and braking functions $F_y(\alpha)$ and $F_x(s)$. This is done later. It is important to note that the friction ellipse is not a tire model. Rather, it is an idealized graphical display of the operating limit for resultant tire forces for any combination of steering and braking. More than one method exists for developing the resultant tire force for combined steering and braking. One, The Nicolas-Comstock-Brach method, is shown in the next Section; others are given by [Pottinger, et al. and Schuring, et al.] and [Hirschberg].

SIMULATION TIRE MODELS

Different tire force models exist and at least one review has been written [Gäfvert, M. and J. Svedenius], but the equations of the models most commonly used in the field of accident reconstruction have not apparently been cataloged. The following is a collection of the equations of tire force models used in three vehicle dynamics simulation software packages common in accident reconstruction.

VCRware Tire Model: The longitudinal and lateral tire force equations for this simulation software are modeled using a subset of the BNP equations [Pacejka]. Equation 7 gives the longitudinal force, $F_x(s)$, for braking alone with no steering ($\alpha = 0$). Figure 4 shows an example of a normalized plot of the longitudinal tire force with example BNP parameter values of $u = s$, $B = 1/15$, $C = 1.5$, $D = 1.0$, $E = 0.30$, $K = 100.0$ and where the slope is

$$\frac{F_x^2\left[F_x(s),F_y(\alpha),\alpha,s\right]}{F_x^2(s)}+\frac{F_y^2\left[F_x(s),F_y(\alpha),\alpha,s\right]}{F_y^2(\alpha)}=1 \quad (3) \qquad \frac{F_x^2(\alpha,s)}{F_x^2(s)}+\frac{F_y^2(\alpha,s)}{F_y^2(\alpha)}=1 \quad (4)$$

$$\frac{F_x^2(\alpha,s)}{\mu_x^2F_z^2}+\frac{F_y^2(\alpha,s)}{\mu_y^2F_z^2}<1 \quad (5) \qquad \mu=\frac{\mu_x\mu_y}{\sqrt{\mu_x^2\sin^2\alpha+\mu_y^2\cos^2\alpha}} \quad (6)$$

$$F_x(s)=D\sin\left\{C\tan^{-1}\left[B(1-E)Ks+E\tan^{-1}(BKs)\right]\right\} \quad (7)$$

$$F_y(\alpha)=D\sin\left\{C\tan^{-1}\left[B(1-E)K\frac{2\alpha}{\pi}+E\tan^{-1}(BK\frac{2\alpha}{\pi})\right]\right\} \quad (8)$$

$$F_x(\alpha,s)=\frac{F_x(s)F_y(\alpha)s}{\sqrt{s^2F_y^2(\alpha)+F_x^2(s)\tan^2\alpha}}\frac{\sqrt{s^2C_a^2+(1-s)^2\cos^2\alpha F_x^2(s)}}{sC_\alpha} \quad (9)$$

$$F_y(\alpha,s)=\frac{F_x(s)F_y(\alpha)\tan\alpha}{\sqrt{s^2F_y^2(\alpha)+F_x^2(s)\tan^2\alpha}}\frac{\sqrt{(1-s)^2\cos^2\alpha F_y^2(\alpha)+C_s^2\sin^2\alpha}}{C_s\sin\alpha} \quad (10)$$

the braking coefficient $C_s = BCDK$. Equation 8 gives the lateral steering force, $F_y(\alpha)$, for no braking ($s = 0$). Figure 5 shows a sample normalized lateral force with BNP parameter values of $u = 2\alpha/\pi$: $B = 8/75$, $C = 1.5$, $D = 1.0$, $E = 0.60$, $K = 100.0$ and the lateral stiffness coefficient is $C_\alpha = BCDK$.

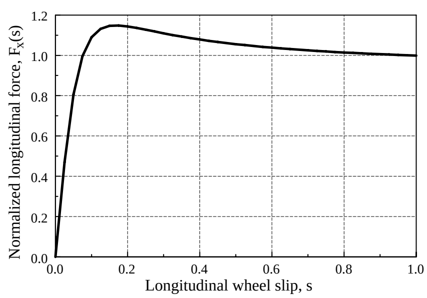

Figure 4. BNP longitudinal force as a function of wheel slip, *s*, VCRware.

For a wheel with a braking force, $F_x(s)$, and a lateral force, $F_y(\alpha)$, the longitudinal force for combined steering and braking, $F_x(\alpha,s)$, is determined in VCRware using the Nicolas-Comstock-Brach, (NCB) equations [Brach & Brach (2000) and Brach & Brach (2005)]. It is given by Eq 9. For a wheel with a braking force, $F_x(s)$, and a lateral force, $F_y(\alpha)$, the lateral force for combined steering and braking, $F_y(\alpha,s)$, is determined using the NCB equation and is given by Eq 10. When plotted on axes of $F_x(s)$ and $F_y(\alpha)$, the NCB equations take the form of a tire force ellipse such as in Fig 3 that depends on the functions $F_x(s)$ and $F_y(\alpha)$. Three-dimensional surface plots of the VCRware tire model are illustrated in Appendix A.

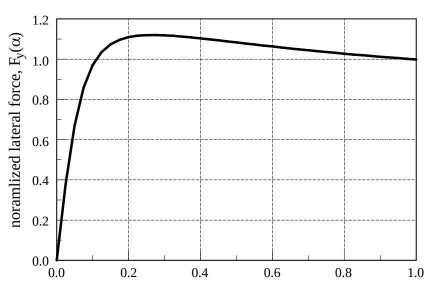

Figure 5. BNP lateral tire force as a function of normalized sideslip, 2α/π, VCRware.

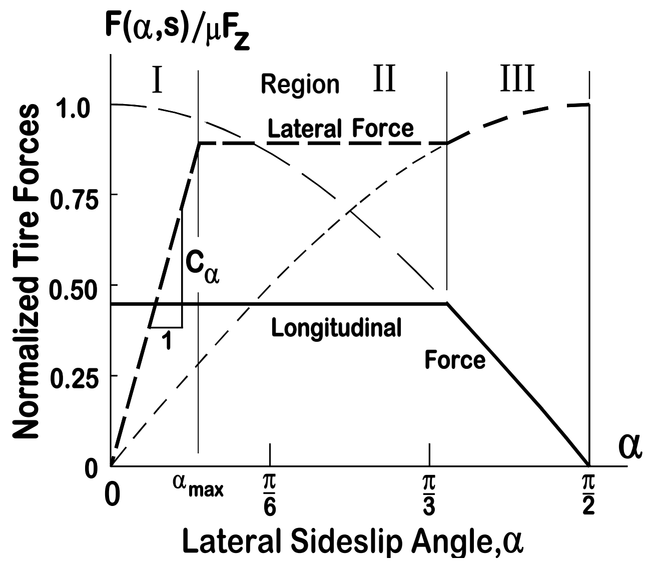

Figure 6. Diagram of longitudinal and lateral tire forces, PC-Crash.

Not all tire models have proper limiting behavior as the wheel slip, s, approaches its limits, 0 and 1, and as the sideslip angle, α, approaches its limits, 0 and $\pi/2$; such behavior must be verified. This is done for the NCB equations in Appendix B.

PC-Crash Linear Tire Force Model: PC-Crash allows the use of two tire models, the Linear Tire Force model and the TM-Easy Tire Force model. The Linear Tire model can be described as follows.

Instead of using the wheel slip parameter, s, the PC-Crash simulation requires an input value of a constant magnitude of applied braking force with a force level, F_b, or an acceleration force magnitude, F_a. A force specified as a fraction of the wheel normal force can alternatively be supplied. For no steering the longitudinal accelerating force, is specified as $F_x = F_a$, and the longitudinal braking force is $F_x = -F_b$. The PC-Crash vehicle dynamic simulation uses a bilinear lateral tire force as shown in Fig 6. The initial linear portion represents a sideslip coefficient of C_α sometimes referred to as the sideslip stiffness.

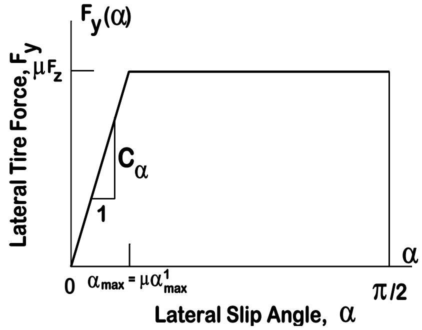

Figure 7. Lateral tire force, Linear Tire Model, PC-Crash.

The lateral force becomes constant at $\alpha = \alpha_{max}$, where the lateral force reaches its maximum value μF_z. For the PC-Crash protocol, $\alpha_{max} = \mu\alpha^1_{max}$, where α^1_{max} is the saturation angle for $\mu_y = 1$. For this notation, the tire sideslip coefficient is computed as $C_\alpha = \mu F_z/\alpha^1_{max}$. For no longitudinal force, $s = 0$, ($F_a = F_b = F_x = 0$) the lateral tire force is defined by Eq 11 and 12. For a wheel with braking force $F_x(\alpha,s) = F_b$ the lateral force is computed using the friction ellipse as given in Eq 13 where the longitudinal force is adjusted for the condition of locked wheel skidding as shown in Eq 14. For combined steering and braking, the PC-Crash Linear Tire Model can be described in three regions (see Fig 6). Region I is when the side force increases linearly with α, Eq 15. Region II is when the side force is said to be saturated and the lateral force is computed using the friction ellipse, Eq 16. Finally, Region III is for locked wheel sliding, as shown in Eq 17. These regions are shown in Fig 6 and are plotted on the friction ellipse in Fig 8. As the sideslip angle, α, increases from 0 to α_{max}, $F_y(\alpha,s)$ goes from (0,0) to point A. The magnitude of the lateral force, $F_y(\alpha,s)$, at point A is determined by F_b and Eq 16. Note that in Region II, while the sideslip angle increases from α_{max} to some value greater than α_{max} as shown in Fig 7, the resultant force at the patch does not change. Thus Region II, for which α varies from α_{max} to some value greater than α_{max}, is concentrated at a single point, B, on the tireforce diagram in Fig 8. In Region III $F_y(\alpha,s)$ goes from point B to point C (as α continues to increase) along the friction ellipse. From Eq 17 note that for Region II (point B), Eq 18 is satisfied. All of this implies that throughout Region II the PC-Crash Linear tire force model gives a lateral force at the friction limit. Although the direction of $F_y(\alpha,s)$ is along the slip direction, the magnitude of the resultant tire force is equal to a fully skidding tire, μF_z. A plot of $F_y(\alpha,s)$ for the PC-Crash tire model is given in Appendix A.

TM-Easy Tire Model [Hirschburg, et al.]: The TM-Easy model is developed for three dimensional vehicle motion. However all of the following discussion is for zero camber and negligible contact moments. According to notes on vehicle dynamics [Rill]. TM-Easy defines longitudinal slip and lateral slip different than above.

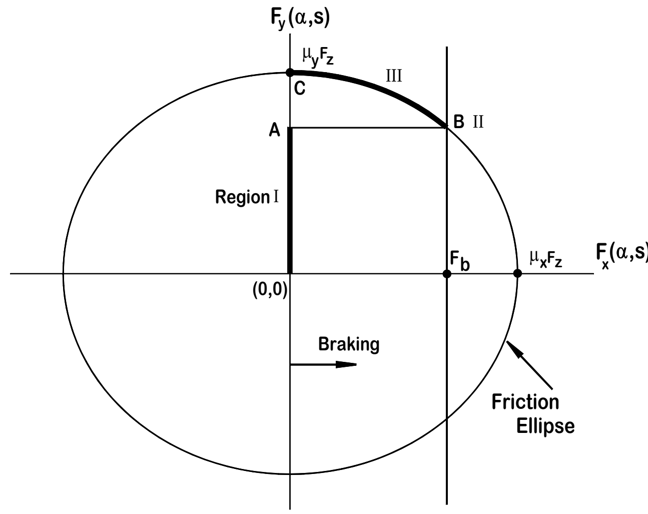

Figure 8. Diagram of lateral and longitudinal tire forces for combined steering and braking, PC-Crash.

Longitudinal slip, s_x, is defined as in Eq 19. TM-Easy lateral slip is defined as in Eq 20. The consequences of normalizing slip to the wheel angular velocity is for TM-Easy that $0 \le s_x \le \infty$, $0 \le s_y \le \infty$ and (for combined steering and braking) that s_x and s_y are coupled to s (Eq 2) and α (Eq 1), as given in Eq 21 through 25. The TM-easy model specifies that beyond a certain, finite value of slip s_{xf}, full sliding occurs. The model can characterize a maximum longitudinal force by specifying maximum values of the force with its corresponding slip (s_{xm}, F_{xm}). Figure 9 shows the longitudinal force F_x as a function of the longitudinal slip s_x. A full description of the model requires that three pieces of information be provided to define the shape of the $F_x(s_x)$ curve: an initial slope, C_x,

$$F_y(\alpha) = -\mu F_z \alpha / \mu\alpha^1_{\max} \tag{11}$$

$\alpha_{max} < \alpha < \pi/2$:

$$F_y(\alpha) = \mu F_z \tag{12}$$

$$F_y(\alpha,s) = \min\left[\mu F_z \frac{\alpha}{\alpha_{\max}}, \sqrt{(\mu F_z)^2 - F_x^2(\alpha,s)}\right] \tag{13}$$

$$F_x(\alpha,s) = \min\left[F_b, \mu F_z \cos\alpha\right] \tag{14}$$

$$F_y(\alpha,s) = \mu F_z \frac{\alpha}{\alpha_{\max}} \tag{15}$$

$$F_y(\alpha,s) = \sqrt{(\mu F_z)^2 - F_b^2} \tag{16}$$

$$F_y(\alpha,s) = \mu F_z \sin\alpha \tag{17}$$

$$\sqrt{F_y^2(\alpha,s) + F_b^2} = \mu F_z \tag{18}$$

the maximum value of the force and its associated slip value (s_{xm}, F_{xm}), and the value of the force at full sliding and its associated slip value (s_{xf}, F_{xf}). The curve for the lateral force, $F_y(s_y)$, can similarly be defined using slope, C_y, maximum parameters (s_{ym}, F_{ym}) and full-sliding parameters (s_{yf}, F_{yf}).

The process outlined above defines the shape of the curve for the longitudinal force in the absence of

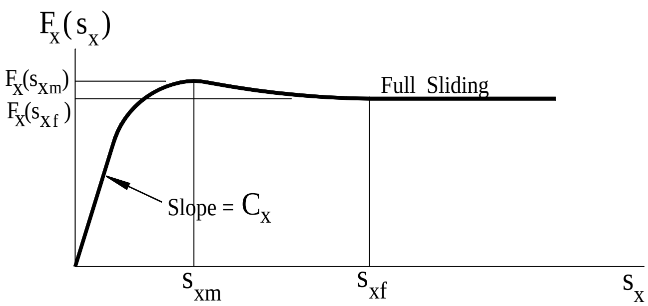

Figure 9. Longitudinal tire force, TM-Easy model.

lateral slip, $F_x(s_x)$, and the curve for the lateral force in the absence of longitudinal slip, $F_y(s_y)$. The force for combined braking and steering, $F(s_x,s_y)$, is formulated by the TM-Easy model through the following process. A generalized slip variable, s_{xy}, which treats the longitudinal and lateral slip vectorially, is defined by Eq 26 where quantities $\hat{s}_x$ and $\hat{s}_y$ are normalized slip variables and are defined by Eq 27 and 28. Equations 29 through 34 define additional parameters. A generalized tire force, $F(s_x,s_y)$ is now described in each of the three intervals by a broken rational function, a cubic polynomial and a constant F_f and given in Eq 35, 36 and 37. Finally, the longitudinal and lateral force components, Eq 38 and 39; these are determined individually from the projections in the longitudinal and lateral directions, using φ, given by Eq 34. Three-dimensional surface plots of the longitudinal and lateral tire forces for combined steering and braking for the TM-Easy model are given in Appendix A.

SMAC Tire Model [HVE and m-smac]: For braking, SMAC does not use the wheel slip variable, *s*, but the simulation user is asked to specify the value of a constant braking force, *T*, which can be defined as a percentage of the available friction force at each wheel. The longitudinal tire force, F_x, is given by Eq 40 through 44 for the different variations of braking and acceleration.

$$s_x = \frac{V_{px}}{R\omega} \quad (19)$$

$$s_y = \frac{V_y}{R\omega} \quad (20)$$

$$s(s_x,s_y) = \frac{V_{px}}{V_x} = \frac{V_x - R\omega}{V_x} \quad (21)$$

$$s(s_x,s_y) = 1 - \frac{R\omega}{V_{px}+R\omega} = \frac{R\omega}{s_x R\omega + R\omega} = \frac{s_x}{1+s_x} \quad (22)$$

$$\alpha(s_x,s_y) = \tan^{-1}\left(\frac{v_y}{v_x + R\omega}\right) = \tan^{-1}\left(\frac{s_y}{1+s_x}\right) \quad (23)$$

$$s_x(s,\alpha) = \frac{s}{1-s} \quad (24)$$

$$s_y(s,\alpha) = \frac{\tan\alpha}{1-s} \quad (25)$$

$$s_{xy} = \sqrt{\left(\frac{s_x}{\hat{s}_x}\right)^2 + \left(\frac{s_y}{\hat{s}_y}\right)^2} \quad (26)$$

$$\hat{s}_x = \frac{s_{xm}}{s_{xm}+s_{ym}} + \frac{F_{xm}/C_x}{F_{xm}/C_x + F_{ym}/C_y} \quad (27)$$

$$\hat{s}_y = \frac{s_{ym}}{s_{xm}+s_{ym}} + \frac{F_{ym}/C_y}{F_{xm}/C_x + F_{ym}/C_y} \quad (28)$$

$$C = \sqrt{\left(C_x \hat{s}_x \cos\varphi\right)^2 + \left(C_y \hat{s}_y \sin\varphi\right)^2} \quad (29)$$

$$s_m = \sqrt{\left(\frac{s_{xm}}{\hat{s}_m}\cos\varphi\right)^2 + \left(\frac{s_{ym}}{\hat{s}_m}\sin\varphi\right)^2} \quad (30)$$

$$F_m = \sqrt{\left(F_{xm}\cos\varphi\right)^2 + \left(F_{ym}\sin\varphi\right)^2} \quad (31)$$

$$s_f = \sqrt{\left(\frac{s_{fx}}{\hat{s}_x}\cos\varphi\right)^2 + \left(\frac{s_{fy}}{\hat{s}_y}\sin\varphi\right)^2} \quad (32)$$

$$F_f = \sqrt{\left(F_{xf}\cos\varphi\right)^2 + \left(F_{yf}\sin\varphi\right)^2} \quad (33)$$

$$\cos\varphi = \frac{s_x/\hat{s}_x}{s_{xy}} \quad \text{and} \quad \sin\varphi = \frac{s_y/\hat{s}_y}{s_{xy}} \quad (34)$$

$$F(s_x,s_y) = \frac{\sigma s_m C}{1+\sigma\left(\sigma + F_f \frac{s_m}{F_m} - 2\right)}, \quad \sigma = \frac{s_{xy}}{s_m}, \quad 0 \le s_{xy} \le s_m \quad (35)$$

$$F(s_x,s_y) = F_m - (F_m - F_f)\sigma^2(3-2\sigma), \quad \sigma = \frac{s_{xy}-s_m}{s_f - s_m}, \quad s_m \le s_{xy} \le s_f \quad (36)$$

$$F(s_x,s_y) = F_f, \; s_{xy} > s_f \quad (37)$$

$$F_x(s_x,s_y) = F(s_x,s_y)\cos\varphi \quad (38)$$

$$F_y(s_x,s_y) = F(s_x,s_y)\sin\varphi \quad (39)$$

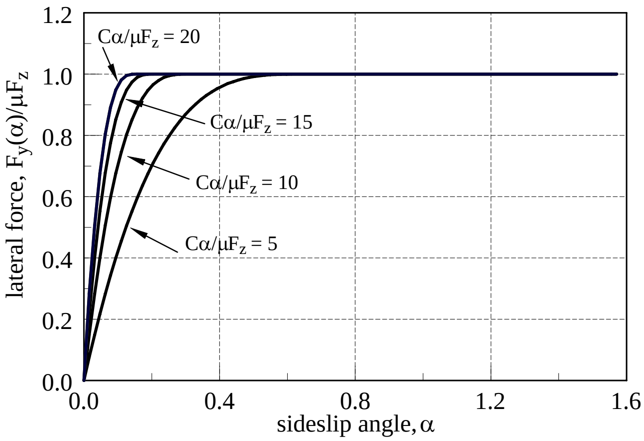

Figure 10. Lateral tire force as a function of sideslip, SMAC.

For the lateral force, SMAC uses a nondimensional variable $\bar{\beta}$, Eq 45, based on the Fiala tire model [EDSMAC, Brach & Brach (2005)] and defines the lateral force $F_y(\alpha)$ by Eq 46 and 47. $F_y(\alpha)$ is plotted in Fig 10 for typical values of $C_\alpha / \mu F_z$.

For a wheel simultaneously steered ($\alpha > 0$) and braked ($T > 0$) the longitudinal tire force, $F_x(\alpha,s)$, is computed by Eq 48 or 49, where the latter case corresponds to locked wheel skidding. For combined braking and steering, the lateral tire force, $F_y(\alpha,s)$, is computed using the longitudinal force, $\bar{\beta}$, newly defined by Eq 50 and the friction ellipse. Then for $\bar{\beta}$, Eq 51 or 52 give $F_y(\alpha,s)$. Equation 52 implies that for $|\bar{\beta}| \geq 3$ the resultant tire force lies on the friction ellipse, as given by Eq 53 and that the SMAC tire force model gives a lateral force at the friction limit for combined steering and braking (before locked wheel sliding occurs). Although the direction of the lateral force, $F_y(\alpha,s)$, is along theslip direction, the magnitude of the resultant tire force equals that of a fully skidding tire.

For braking:

$$T = 0\ (s = 0), \quad F_x(T) = 0 \tag{40}$$

$$0 < T \leq \mu F_z, \quad F_x(T) = -T \tag{41}$$

$$T > \mu F_z, F_x(T) = -\mu F_z \tag{42}$$

For acceleration

$$|T| \leq \mu F_z, \quad F_x(T) = T \tag{43}$$

$$|T| > \mu F_z, \quad F_x(T) = \mu F_z \tag{44}$$

$$\bar{\beta} = \bar{\beta}(\alpha) = \frac{C_\alpha \alpha}{\sqrt{\mu^2 F_Z^2}} \tag{45}$$

$$\text{For } |\bar{\beta}| < 3, \; F_y(\alpha) = \mu F_Z \left[\bar{\beta} - \frac{\bar{\beta}|\bar{\beta}|}{3} + \frac{\bar{\beta}^3}{27} \right] \tag{46}$$

$$\text{For } |\bar{\beta}| \geq 3, \; F_y(\alpha) = \mu F_Z \tag{47}$$

$$\text{For } F_X(T) \leq \mu F_Z \cos\alpha, \; F_X(\alpha,s) = T \tag{48}$$

$$\text{For } F_X(T) > \mu F_Z \cos\alpha, \; F_X(\alpha,s) = \mu F_Z \cos\alpha \tag{49}$$

$$\bar{\beta} = \bar{\beta}(\alpha) = \frac{C_\alpha \alpha}{\sqrt{\mu^2 F_Z^2 - F_X^2(\alpha,s)}} \tag{50}$$

For $|\bar{\beta}| < 3$,

$$F_y(\alpha,s) = \sqrt{\mu^2 F_Z^2 - F_X^2(\alpha,s)} \left(\bar{\beta} - \frac{1}{3}\bar{\beta}|\bar{\beta}| + \frac{1}{27}\bar{\beta}^3 \right) \tag{51}$$

For $|\bar{\beta}| \geq 3$,

$$F_y(\alpha,s) = \sqrt{\mu^2 F_Z^2 - F_X^2(\alpha,s)} \tag{52}$$

$$\sqrt{F_X^2(\alpha,s) + F_y^2(\alpha,s)} = \mu F_Z \tag{53}$$

A three-dimensional surface plot of the SMAC $F_y(\alpha,s)$ using Eq 51 through 53 is included in Appendix A.

SIMON Tire Model [HVE]: SIMON [EDC] uses a semi-empirical tire model which is based upon the HSRI tire model [MacAdam, et al.]. The principle behind the HSRI tire model is that the tire forms a rectangular contact patch which can be divided into two regions, consisting of a no-slip region and a sliding region. The relative size of the two regions is dependant upon the longitudinal and lateral slip values, s and α, the sliding frictional drag coefficient, μ, and the initial slopes, C_s and C_α, of the linear tire force curves,.

The first step in determining the SIMON tire forces is to determine an equivalent frictional drag coefficient, μ', that depends on the slip, s, and is calculated from the directional sliding frictional drag coefficients, μ_x and μ_y The coefficient, μ' is found using a fitting procedure whereby,

$$a = (1 - s_p)^2 (1 + s_p) \tag{54}$$

$$b = (1 - s_p)\left(\mu_X (s_p + 2) - \mu_p (2 s_p + 1) \right) \tag{55}$$

$$c = (\mu_X - \mu_p)\mu_X \tag{56}$$

$$B = \frac{-b + \sqrt{b^2 - 4ac}}{2a} \tag{57}$$

$$A = \mu_X + B \tag{58}$$

$$C = \mu_X + B(1 - s_p) \tag{59}$$

and

$$\mu' = A - Bs \tag{60}$$

In these equations, μ_p is the ratio of longitudinal tire force $F_x(s)_{max}/F_z$ and s_p is the slip at $F_x = F_x(s)_{max}$. A variable D_t is defined as,

$$D_t = \sqrt{(C_s s)^2 + (C_\alpha \sin\alpha)^2} \tag{61}$$

where s is the longitudinal tire slip and α is the sideslip angle. After calculating μ', a fraction, X_s/L, representing the portion of the total contact patch that is not slipping, where L is the length of the rectangular tire patch, is defined as:

$$\frac{X_S}{L} = \frac{\mu' F_Z}{2 D_t}(1 - |s|), \; 0 \leq \frac{X_S}{L} \leq 1 \tag{62}$$

The equations for combined steering and braking/acceleration follow. The equations for steering

$\underline{X_s / L = 1}$:

$$F_X(\alpha,s) = C_S \frac{s}{1-|s|} \tag{63}$$

$$F_y(\alpha,s) = -\frac{C_\alpha \sin\alpha}{1-|s|} \tag{64}$$

$\underline{X_s / L < 1}$:

$$F_X(\alpha,s) = C_S s \left(\frac{\mu' F_Z}{2D_t}\right)^2 (1-|s|) + \mu' F_Z \left(1-\frac{X_S}{L}\right)\left(\frac{s}{\sqrt{s^2+\sin^2\alpha}}\right) \tag{65}$$

$$F_y(\alpha,s) = -C_\alpha \sin\alpha \left(\frac{\mu' F_Z}{2D_t}\right)^2 (1-|s|) - \mu' F_Z \left(1-\frac{X_S}{L}\right)\left(\frac{\sin\alpha}{\sqrt{s^2+\sin^2\alpha}}\right) \tag{66}$$

alone and braking alone can be found by substituting s = 0 and α = 0 into the equations, respectively. For combined braking and steering, three-dimensional surface plots of $F_x(\alpha,s)$ and $F_x(\alpha,s)$ are in Appendix A.

The sine functions in the range $-\pi \leq \alpha \leq \pi$ as used in the above equations for the SIMON model were changed from tangent functions in the original HSRI model. EDC is now investigating the full effects of this change. In addition, various empirical curves from measured tire parameters are built into the HVE software that make the tire characteristics tire specific and functions of load and speed. However, the user has the ability to enter other tire characteristics or to use setup tables based upon a specific tire tests. The full SIMON tire model considers the effects that camber stiffness has on the lateral tire forces.

DISCUSSION AND CONCLUSIONS

The primary purpose of this paper is to demonstrate that different tire models exist, to describe them in as much detail as possible and to indicate which simulation programs (used in accident reconstruction applications) use which tire models.

Alternative methods exist [Kiefer, et al., 2005, 2007] to estimate the combined effects of initial translational and rotational velocities on the trajectory of a vehicle to rest following impact that do not use tire force models. Such methods do not have the potential of simulating different tire properties and accident reconstruction conditions such as partial braking, powertrain drag, rolling wheel drag and/or the effects of an individually locked wheel or wheels. It is necessary to use a vehicle dynamic simulation program for modeling such conditions. Despite the greater potential for accuracy, the uncertainty due to different tire models used in the simulation software cannot be overlooked. Differences do exist. All other things being equal, the more accurate the tire model, that is, the closer the tire model is to experimentally measured tire performance, the more accurate the simulation. In this paper, tire models that incorporate the wide ranges of s and α typically found in accident reconstruction applications are presented. Any differences in simulation results can be described as model uncertainty. If all of the simulations contain identical Newton's equations of motion and integrate them with the same precision. The modeling uncertainty can be attributed primarily to the tire models, although differences in modeling of other components may exist.

Tire Force Models: For combined braking and steering of an individual wheel, the PC-Crash Linear Tire Force model is based on the process of first specifying the longitudinal (braking or accelerating) force, representing the lateral (steering) force with a bilinear curve and the use of the friction ellipse to compute the resultant tire force. For combined braking and steering of an individual wheel, the SMAC tire force model (both EDSMAC4 and m-smac) is based on the process of first specifying the longitudinal (braking or accelerating) force, using the Fiala model for the lateral (steering) force and the use of the friction ellipse to compute the resultant tire force for combined steering and braking. The VCRware tire force model uses BNP equations with different parameters for the longitudinal and lateral forces and then uses the NCB equations for combined steering and braking. PC-crash allows the use of the Linear Tire Model or an alternative called the TM-Easy Model. The TM-Easy Model is based on a resultant wheel slip vector for combined steering and braking. The SIMON tire force model is based on a modified HSRI Tire Model.

For the tire models covered in this paper two categories can be established. One category uses a specified level of braking (or acceleration) to establish the longitudinal tire force and the friction ellipse to calculate the combined longitudinal and lateral tire force components for combined steering and braking (PC-Crash Linear and SMAC Tire Models). The second category uses the direction of the wheel slip vector or slip velocity at the tire patch to determine the longitudinal and lateral tire force components for combined steering and braking (VCRware, PC-Crash TM-Easy and SIMON tire models). Within each category, however, these models use different forms of equations to model the lateral tire forces (for no braking).

It was shown that for relatively low sideslip angles, the use of the friction ellipse as part of the tire model produces resultant forces equal in magnitude to a fully sliding tire. Some [Gäfvert & Svedenius] object to this feature because it is thought it introduces the friction limit force (sliding force) before sliding occurs. However, the use of the friction ellipse can actually *under-predict* actual combined tire forces. This is because the performance of models also depends on the functions used to represent the steering-alone and braking-alone curves, $F_x(s)$ and $F_y(\alpha)$. Experimentally measured tire forces [Salaani] almost always exceed the locked-wheel skid force, μF_z, over some (early) regions of slip. Figure 11 is a plot of normalized BNP-NCB combined tire forces (which reflect measured characteristics) plotted on the friction ellipse coordinate system. The "friction ellipse" corresponding to the BNP-NCB tire forces is the locus of points of the curves for all values of α that lie a maximum radial distance from the origin (0,0). The friction ellipse for combined forces whose $F_x(s)$ and $F_y(\alpha)$ tire force curves do not exceed μF_z is given by the dashed curve in Fig 11. As seen, the idealized friction ellipse can result in combined tire forces well below measured values.

It is clear that the mathematical complexity of the different tire models varies considerably. This feature in combination with a comparison of the models to experimental data should determine which model provides a more accurate prediction of the tire forces.

ACKNOWLEDGMENTS

The authors appreciate the cooperation of MEA Forensic Engineers and Scientists and for providing data, information and guidance with respect to the PC-Crash linear tire model. The assistance of Terry Day of Engineering Dynamics Corporation is also gratefully appreciated. Finally, Prof. Dr. Georg Rill provided help and information with the formulation of the TM-Easy tire model.

The assistance of Ron Jadischke, McCarthy Engineering, is gratefully acknowledged for formulating the equations of the SMAC and SIMON models.

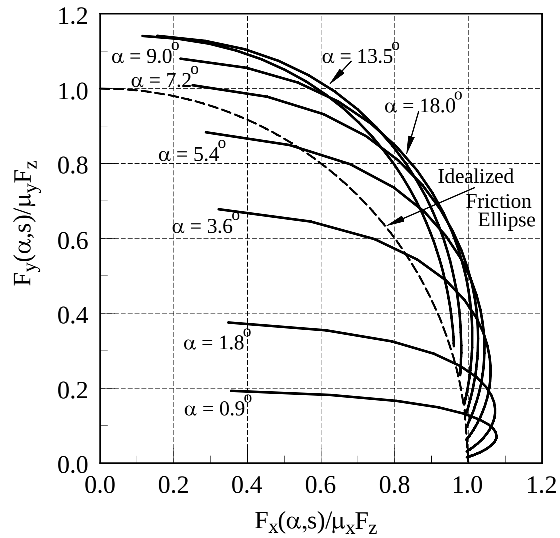

Figure 11. Normalized BNP-NCB combined tire forces (solid curves) and the normalized friction ellipse (dashed curve) for $\mu_x = \mu_y$.

REFERENCES

ADAMS, http://www.mscsoftware.com/products/adams.cfm

Allen, R. W., R. Magdeleno, T. Rosenthal, D. Klyde and J. Hogue, "Tire Modeling Requirements for Vehicle Dynamics Simulation", Paper No. 950312, SAE, Warrendale, PA, 1995.

Brach, Raymond and Matthew Brach, "Tire Forces: Modeling the Combined Braking and Steering Forces", Paper 2000-01-0357, SAE, Warrendale, PA, 2000.

Brach, Raymond and Matthew Brach, *Vehicle Accident Analysis and Reconstruction Methods*, SAE, Warrendale, PA, 2005.

Car-Sim, http://www.carsim.com/

Daily, J., N. Shigemura and J. Daily, *Fundamentals of Traffic Crash Reconstruction*, *Volume 2 of the Traffic Crash Reconstruction Series* , IPTM, Jacksonville, FL, 2006.

EDC, (Engineering Dynamics Corporation, *SIMON Simulation Model*, 5th Edition", January 2006.

Fricke, L., (1) *Traffic Accident Reconstruction*, Northwestern University , Evanston, IL, 1990.

Fricke, L., (2) *Traffic Accident Reconstruction*, Volume 2, *Traffic Accident Investigation Manual*, Northwestern University , Evanston, IL, 1990.

Gäfvert, M. and J. Svedenius, "Construction of Novel Semi-Empirical Tire Models for Combined Braking and Cornering", ISSN 0280-5316, Lund Institute of Technology, Sweden, 2003.

Guo, Konghui and Lei Ren, "A Unified Semi-Empirical Tire Model With Higher Accuracy and Less Parameters", Paper 1999-01-0785, SAE International, Warrendale, PA, 1999.

Han, I. and S-U Park, Inverse Analysis of Pre- and Post-Impact Dynamics for Vehicle Accident Reconstruction, *Vehicle System Dynamics*, V 36, **6**, pp 413-433, 2001.

Hölscher, H., M. Tewes, N. Botkin, M. Lohndorf, K-H. Hoffman, and E. Quandt - Modeling of Pneumatic Tires by a Finite Element Model for the Development of a Tire Friction Remote Sensor, preprint submitted to *Computers and Structures*.

Hirschberg, W., G. Rill and H.Weinfurter, "User-Appropriate Tyre-Modelling for Vehicle Dynamics in Standard and Limit Situations," *Vehicle Systems Dynamics*, Vol. 38, No. 2, pp 103-125.

HVE, http://www.edccorp.com/products/hve.html

Keifer, O., P. Reckamp, T. Heilmann and P. Layson, “A Parametric Study of Frictional Resistance to Vehicular Rotation Resulting From a Motor Vehicle Impact”, Paper 2005-01-1203, SAE, Warrendale, PA, 2005.

Keifer, O., P. Conte and B. Reckamp, *Linear and Rotational Motion Analysis in Traffic Crash Reconstruction*, IPTM, Jacksonville, FL, 2007.

MacAdam, C., P. S. Fancher, T. H. Garrick, T. D. Gillespie, “A Computerized Model for Simulating the Braking and Steering Dynamics of Trucks, Tractor-Semitrailers, Doubles and Triples Combinations”, Highway Safety Research Institute., The University of Michigan (UM-HSRI-80-58).

Martinez, J. E. and R. J. Schleuter, A Primer on the Reconstruction and Presentation of Rollover Accidents, Paper 960647, SAE International, Warrendale, PA, 1996.

McHenry, R., “Computer Program for Reconstruction of Highway Accidents”, Paper 730980, SAE Warrendale, PA, 1973

m-smac, http://www.mchenrysoftware.com

Orlowski, K. R., E. A. Moffatt, R. T. Bundorf and M. P. Holcomb, “Reconstruction of Rollover Collisions”, Paper 890857, SAE International, Warrendael, PA, 1987.

Pacejka, Hans, *Tire and Vehicle Dynamics*, SAE, Warendale, PA, 2002.

PC-Crash, http://www.meaforensic.com/technical/pc_crash.html

Pottinger, M. G., Pelz, W., and Falciola, G., "Effectiveness of the Slip Circle, "Combinator", Model for Combined Tire Cornering and Braking Forces When Applied to a Range of Tires", SAE Paper 982747, Warrendale, PA 15096.

Rill, G, *Vehicle Dynamics Lecture Notes*, University of Applied Sciences, Hochschule für Technik Wirtschaft Soziales, Germany, 2007.

Salaani, K., “Analytical Tire Forces and Moments Model with Validated Data”, Paper 2007-01-0816, SAE International, Warrendale, PA, 2007.

Segal, J. *Highway Vehicle Object Simulation Model*, 4 Volumes (Users Manual, Programmers Manual, Engineering Manual-analysis, and Engineering Manual), 1422 pgs, Calspan Corporation, 1976.

Schuring, D. J., Pelz, W, Pottinger, M. G., 1993, "An Automated Implementation of the ’Magic Formula’ Concept", SAE Paper 931909, Warrendale, PA 15096.

Tönük, E. and Y. S. Ünlüsoy, “Prediction of automobile tire cornering force characteristics by finite element modeling and analysis”, *Computers and Structures*, 79 (2001), pp1219-1232.VCRware, http://www.brachengineering.com/menu.swf

VDANL, http://www.systemstech.com/content/view/32/39/

Appendix A. Three-dimensional plots of Tire Forces of Different Models

Criteria have been published for the proper formulation and performance of tire models for combined steering and braking [Gäfvert, M. and J. Svedenius, Brach & Brach,2000]. These are:

1. The combined force functions, $F_x(\alpha,s)$ and $F_y(\alpha,s)$, should preferably be constructed from pure slip models, $F_x(s)$ and $F_y(\alpha)$, with few additional parameters.
2. The computations involved in the models must be numerically feasible and efficient.
3. The formulas should preferably be physically motivated.
4. The combined force functions, $F_x(\alpha,s)$ and $F_y(\alpha,s)$, should reduce to $F_x(s)$ and $F_y(\alpha)$, for pure cornering or braking,
5. Sliding must occur simultaneously in longitudinal and lateral directions.
6. The resulting force magnitudes should stay within the friction ellipse*.
7. The combined force components should become $F_x(s) = \mu_x F_z \cos \alpha$ and $F_y(\alpha) = \mu_y F_z \sin \alpha$ for conditions of locked wheel skidding.

With these in mind, three-dimensional surface plots of the forces (for combined braking and steering) from the different tire models are presented below. Note that some do not meet all of the above criteria.

Figures 12 through 19 are surface plots of the normalized tire forces for combined braking and steering for all of the models covered in this paper. Figures 12 and 13 are for the BNP-NCB tire model used by VCRware. Figure 14 shows the lateral force from PC-Crash Linear Tire model for values for $0 \leq F_b/\mu F_z \leq 1$ and for $0 \leq \alpha \leq \pi/2$. Figure 15 shows the normalized lateral force from SMAC for $0 \leq T/\mu_x F_z \leq 1$ and for $0 \leq \alpha \leq \pi/2$. The longitudinal forces for these models are not plotted since braking forces are specified as input to the program rather than being calculated as a function of wheel slip. Figures 16 and 17 are the longitudinal and lateral tire forces from the SIMON model. Figures 18 and 19 are the longitudinal and lateral tire force models from the TM-Easy Tire model.

* This is true only when the longitudinal and lateral tire forces do not exceed μFz. As shown in this paper in Figure 11, actual combined resultant tire forces can lie outside the idealized tire force ellipse.

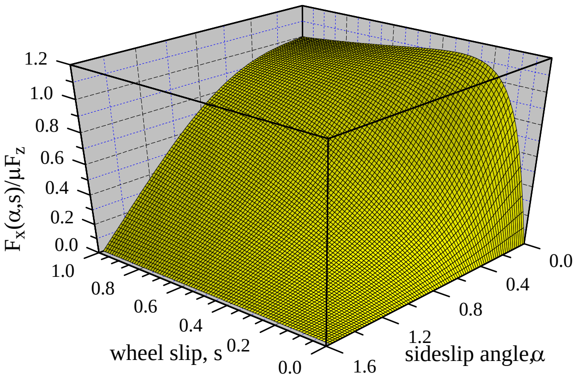

Figure 12. Normalized longitudinal tire force for combined braking and steering, VCRware.

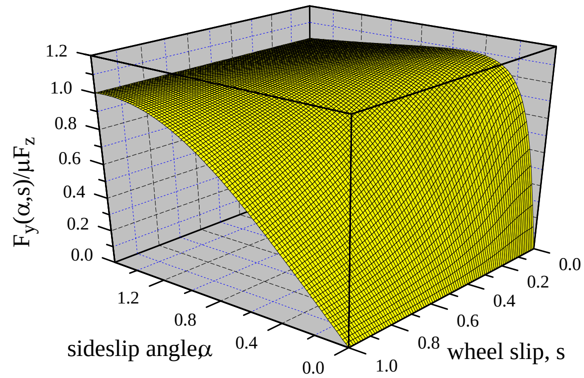

Figure 13. Normalized lateral tire force for combined braking and steering, VCRware.

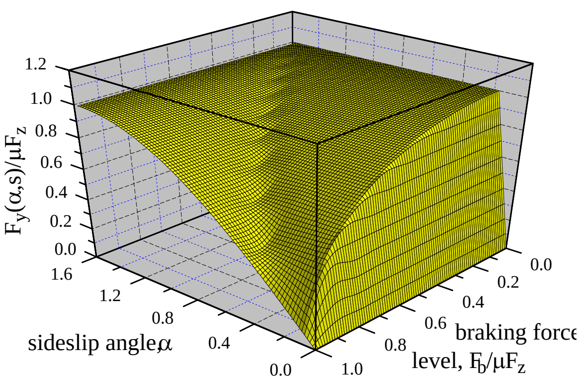

Figure 14. Normalized lateral tire force for combined braking and steering, PC-Crash Linear Tire Model.

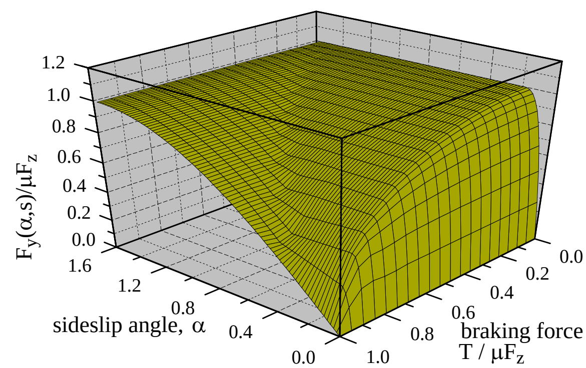

Figure 15. Normalized lateral tire force for combined braking and steering, SMAC.

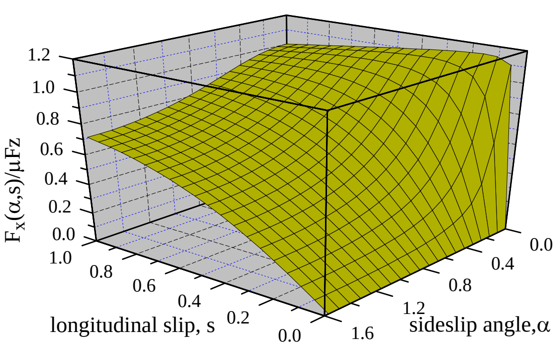

Figure 16. Normalized longitudinal tire force for combined braking and steering, SIMON.

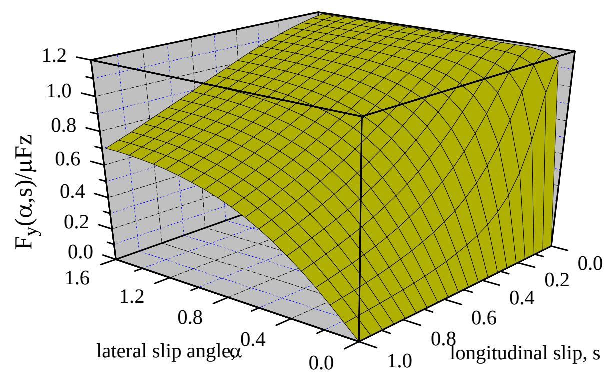

Figure 17. Normalized lateral tire force for combined braking and steering, SIMON.

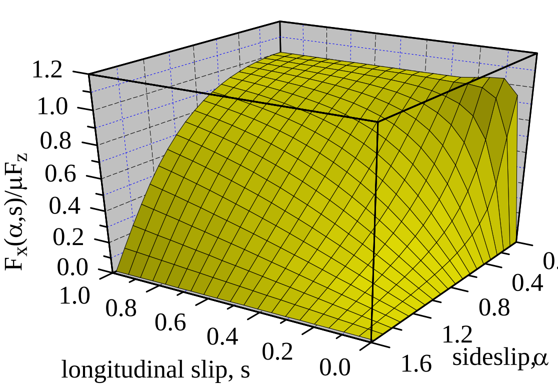

Figure 18. Normalized longitudinal tire force for combined braking and steering, TM-Easy.

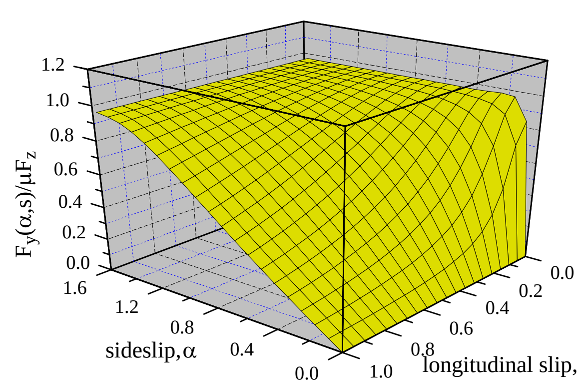

Figure 19. Normalized lateral tire force for combined braking and steering, TM-Easy.

Appendix B. Limiting behavior of the Nicolas-Comstock-Brach combined tire force equations

Not all tire models have proper limiting behavior as the wheel slip, s, approaches its limits, 0 and 1, and as the sideslip angle, α, approaches its limits, 0 and $\pi/2$. Such behavior must be verified. The Nicolas-Comstock-Brach (NCB) equations are given above as Equations 9 and 10. A unique and remarkable feature of these equations is that they can be used to provide the combined tire forces, $F_x(\alpha,s)$ and $F_y(\alpha,s)$, for any pair of longitudinal and lateral tire force equations, $F_x(s)$ and $F_y(\alpha)$, respectively. In this appendix, the NCB equations are examined to ensure that the combined tire forces have the proper limiting behavior as $s \Rightarrow 0,1$ and $\alpha \Rightarrow 0,\pi/2$. These limiting conditions are not unique to the NCB model. All combined-force tire models should satisfy these conditions.

Specifically, eight limiting cases are identified:

1. as $s \Rightarrow 0$, $F_x(\alpha,s) \Rightarrow 0$,
2. as $s \Rightarrow 1$, $F_x(\alpha,s) \Rightarrow \mu_x F_z \cos\alpha$,
3. as $\alpha \Rightarrow 0$, $F_x(\alpha,s) \Rightarrow F_x(s)$,
4. as $\alpha \Rightarrow \pi/2$, $F_x(\alpha,s) \Rightarrow 0$,
5. as $s \Rightarrow 0$, $F_y(\alpha,s) \Rightarrow F_y(\alpha)$
6. as $s \Rightarrow 1$, $F_y(\alpha,s) \Rightarrow \mu_y F_z \sin\alpha$
7. as $\alpha \Rightarrow 0$, $F_y(\alpha,s) \Rightarrow 0$
8. as $\alpha \Rightarrow \pi/2$, $F_y(\alpha,s) \Rightarrow \mu_y F_z$

Case 1. For $s \sim 0$, $(1 - s^2) \sim 1$ and $F_x(s) \sim C_s\, s$. From Eq 9

$$F_x(\alpha,s)|_{s\to 0} = \frac{F_y(\alpha)}{\sqrt{F_y^2(\alpha)+C_s^2\tan^2\alpha}}\, s\, \frac{\sqrt{C_\alpha^2+C_s^2\cos^2\alpha}}{C_\alpha} = 0 \qquad \text{(B-1)}$$

Case 2. For $s = 1$ (locked wheel skidding), $F_x(s)|_{s=1} = \mu F_z$. From Eq 9

a. For large α, $F_y(\alpha) \sim \mu F_z$. From Eq 9

$$F_x(\alpha,s)|_{s\to 1} = \frac{\mu F_z \mu F_z \cos\alpha}{\sqrt{\mu^2 F_z^2\cos^2\alpha+\mu^2 F_z^2\sin^2\alpha}}\, \frac{\sqrt{C_\alpha^2}}{C_\alpha} = \mu F_z\cos\alpha \qquad \text{(B-2)}$$

b. For small α, $\cos\alpha \sim 1$, $\sin\alpha \sim \alpha$ and $F_y(\alpha) \sim C_\alpha \alpha$. For $C_\alpha >> \mu F_z$

$$F_x(\alpha,s)|_{s\to 1} = \frac{1}{\sqrt{1+\frac{\mu^2 F_z^2}{C_\alpha^2}}}\, \mu F_z \sim \mu F_z \qquad \text{(B-3)}$$

Case 3. As $\alpha \Rightarrow 0$, $F_y(\alpha) \approx C_\alpha \alpha$, $\tan\alpha \sim \alpha$, $\cos\alpha \sim 1$. From Eq 9

$$F_x(\alpha,s)|_{\alpha\to 0} = \frac{\sqrt{s^2 C_\alpha^2+(1-s)^2 F_x^2(s)}}{\sqrt{s^2 C_\alpha^2+F_x^2(s)}}\, F_x(s) \qquad \text{(B-4)}$$

a. For $s << 1$

$$F_x(\alpha,s)|_{\alpha\to 0} = F_x(s) \qquad \text{(B-5)}$$

b. For large s ($s \sim 1$) and $\mu_x F_z << C_\alpha$

$$F_x(\alpha,s)|_{\alpha\to 0} = \frac{F_x(s)}{\sqrt{1+\frac{\mu_x F_z^2}{C_\alpha^2}}} \sim \mu F_z \qquad \text{(B-6)}$$

Case 4. As $\alpha \Rightarrow \pi/2$, $\cos\pi/2 = 0$, $\tan\pi/2 \Rightarrow \infty$ from Eq 9

$$F_x(\alpha,s)|_{\alpha\to\pi/2} = \frac{F_x(s)\mu_y F_z s}{\sqrt{s^2\mu_y^2 F_z^2+F_x^2(s)\tan^2\alpha}} = 0 \qquad \text{(B-7)}$$

Case 5. As $s \Rightarrow 0$, $F_x(s) \sim C_s s$. From Eq 10

$$F_y(\alpha,s)|_{s\to 0} = \frac{C_s s F_y(\alpha)}{\sqrt{s^2F_y^2(\alpha)+C_s^2 s^2 \tan^2\alpha}} \frac{\sqrt{F_y^2(\alpha)+C_s^2\tan^2\alpha}}{C_s} = F_y(\alpha) \tag{B-8}$$

Case 6. as $s \Rightarrow 1$, $F_x(s) = \mu F_z$. From Eq 10

$$F_y(\alpha,s)|_{s\to 1} = \frac{1}{\sqrt{\cos^2\alpha + \dfrac{\mu^2F_z^2}{F_y^2(\alpha)}\sin^2\alpha}} \mu F_z \sin\alpha \tag{B-9}$$

a. For small α, $\cos\alpha \sim 1$, $\sin\alpha \sim \alpha$, $F_y(\alpha) \sim C_\alpha \alpha$ and $C_\alpha >> \mu F_z$

$$F_y(\alpha,s)|_{s\to 1} = \mu F_z \sin\alpha \tag{B-10}$$

For large α, $F_y(\alpha) \sim \mu F_z$ and

$$F_y(\alpha,s)|_{s\to 1} = \mu F_z \sin\alpha \tag{B-11}$$

Case 7. For $\alpha \Rightarrow 0$, $F_y(\alpha) = C_\alpha \alpha$. From Eq 10

$$F_y(0,s)|_{\alpha\to 0} = \frac{F_x(s)C_\alpha\alpha}{\sqrt{s^2C_\alpha^2+F_x^2(s)}} \frac{\sqrt{(1-s)^2C_\alpha^2+C_s^2}}{C_s} = 0 \tag{B-12}$$

since as $\alpha \Rightarrow 0$, the numerator $\Rightarrow 0$ but the denominator is bounded.

Case 8. For $\alpha \Rightarrow \pi/2$, $F_y(\alpha) \Rightarrow \mu F_z$. From Eq 10

$$F_y(\alpha,s)|_{\alpha\to\pi/2} = \mu F_z \tag{B-13}$$

The combined NCB forces are shown in Figures 20 and 21 for generic BNP forces and for the full range of wheel slip, *s,* and sideslip, *α*:

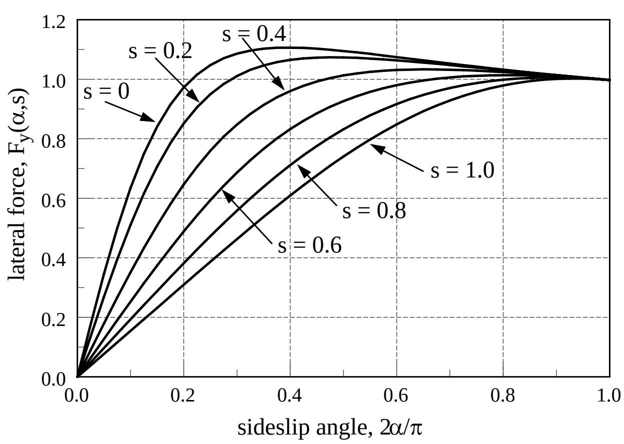

Figure 20. Combined lateral force, BNP-NCB model.

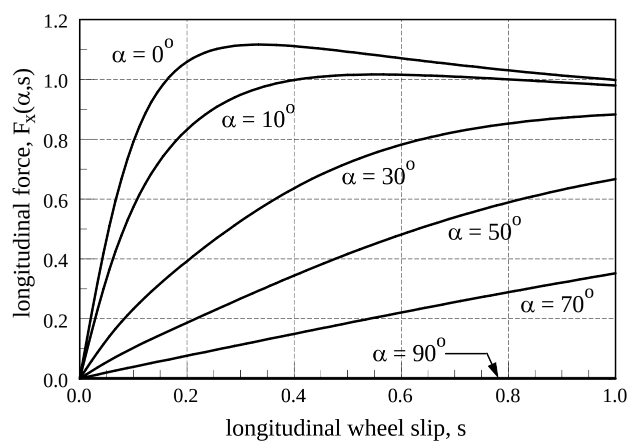

Figure 21. Combined longitudinal force, BNP-NCB model.